Spatiotemporal variation in the distribution of chytrid parasites in diatom host populations

Gsell, A.S.; De Senerpont Domis, L.N.; Naus-Wiezer, S.M.H.; Helmsing, N.R.; Van Donk, E.; Ibelings, B.W.

published in
Freshwater Biology
2013

DOI (link to publisher)
10.1111/j.1365-2427.2012.02786.x

document version
Peer reviewed version

Spatio-temporal variation in the distribution of chytrid parasites in diatom host populations

ALENA S. GSELL*, LISETTE N. DE SENERPONT DOMIS*, SUZANNE M. H. NAUS-WIEZER*, NICO R. HELMSING*, ELLEN VAN DONK*† AND BAS W. IBELINGS*‡

**Department of Aquatic Ecology, Netherlands Institute of Ecology (NIOO-KNAW), Wageningen, The Netherlands*

†*Department of Biology, Palaeoecology, University of Utrecht, Utrecht, The Netherlands*

‡*Department of Aquatic Ecology, EAWAG, Dübendorf, Switzerland*

Correspondence:

Alena S. Gsell, Department of Aquatic Ecology, Netherlands Institute of Ecology (NIOO-KNAW), Droevendaalsesteeg 10, 6708 PB Wageningen, The Netherlands

Email: a.gsell@nioo.knaw.nl

Running head: Spatio-temporal variation in host and parasite populations

Keywords: Host-parasite interaction, lake, phytoplankton, spatio-temporal dynamics, vertical patchiness

SUMMARY

1) Many host-parasite interaction dynamics show distinct seasonality. Parasite population growth and invasion success are generally explained by host density dependence, while the direct influence of environmental factors on parasite life history traits has been underreported.
2) In water bodies, resource availability and environmental conditions change with season (temperature, irradiance and rainfall patterns) and with depth (light, temperature and chemical gradients). Hence, hosts and parasites live in a spatially and temporally variable environment. Such environmental variation leads to structured populations, which in turn have implications for host-parasite interaction dynamics. Nevertheless, time-series data on the vertical distribution of aquatic hosts and their parasites are rare.
3) We present a dataset spanning 1.5 years (2008-2010) of weekly sampling in Lake Maarsseveen (The Netherlands) focussing on the dynamics of the diatom *Asterionella formosa* and its parasite, the chytrid *Zygorhizidium planktonicum*, at four depths. Environmental variables measured included ice cover, temperature, global irradiance, light extinction, pH, soluble reactive silicate, dissolved nitrate and ortho-phosphate.
4) We observed four host blooms, two in early spring and one each in summer and autumn. Each host bloom was followed by a time-lagged parasite epidemic. Blooms and epidemics started in the uppermost water layers and showed a time lag in onset date with increasing depth.
5) Host abundance was related to soluble reactive silicate, global irradiance, Schmidt stability and parasite abundance in the upper 10 m, whereas at 15 m only a relationship with parasite abundance prevailed. Parasite abundance was related to host abundance, light extinction, temperature, soluble reactive silicate, stability and global irradiance within the upper 10 m; again, at 15 m, parasite abundance correlated only with host abundance and disease prevalence.
6) Host vertical distribution was less aggregated during isothermal conditions than during thermal stratification, when host abundance was higher in the mixed, photic epilimnion and lower in the dark, colder hypolimnion. Parasite vertical distribution was patchy most of the year. Parasite epidemics seemed to reduce host vertical patchiness as they impacted higher density patches in the photic zone more strongly, a result of both higher host abundance and favourable environmental conditions for the parasite.

7) Seasonal variability and vertical gradients in biotic and abiotic factors expose host and parasite individuals to different environmental conditions even within a single population. Environmental variability affects parasite transmission rates through changes in host abundance and through changes in the strength and outcome of host-parasite interactions.

Introduction

Many host-parasite dynamics are distinctly seasonal (Altizer et al. 2006). Host distribution, abundance and condition are often explained exclusively by environmental factors while microparasite invasion and spread are generally interpreted as a time-lagged, density-dependent consumer-resource interaction (Arneberg et al. 1998, Ebert et al. 2000, Gerber et al. 2005, Hall et al. 2009). Parasites, however, are also directly affected by environmental conditions either during transmission or, in ectoparasites, during their complete lifecycle (Frost et al. 2008, Krasnov et al. 2010, Laine 2007, Mitchell et al. 2005, Paull and Johnson 2011). If environmental factors indeed play an important role in shaping parasite lifecycles, transmission success and productivity, we risk missing crucial information on host-parasite dynamics when considering host density effects alone.

Parasite invasion success and spread through host populations is often summarized by R_0, the net reproductive rate of the parasite (Anderson and May 1991, Paull and Johnson 2011). R_0 is based on host density and recovery rate and on parasite transmission rate, infectivity and virulence. However, when calculating R_0 it is often assumed that hosts and parasites are distributed homogeneously and interact in equally homogeneous environments (Anderson and May 1991, Keeling and Grenfell 2000). How spatial structuring affects both invasion success and spread of diseases is increasingly incorporated into network-based epidemiological models (Keeling and Eames 2005). Spatially explicit models of host and parasite populations show that host patchiness can limit parasite spread, result in fiercer intraspecific competition than expected in more homogeneously mixed populations (Keeling 1999) and makes parasites more vulnerable to stochastic events (Dangerfield et al. 2009). Detailed descriptions of host-parasite dynamics in spatially and temporally structured environments are needed to provide data for spatially explicit models.

Host-parasite dynamics of *Asterionella formosa* Hassall and the chytrid fungus *Zygorhizidium planktonicum* Canter have been monitored extensively in dimictic Lake Maarsseveen, The Netherlands (Ibelings et al. 2004, Ibelings et al. 2011, Van Donk and Ringelberg 1983). *Asterionella* is a characteristic phytoplankton species of temperate lakes where it is often the dominant spring bloom species (Lund et al. 1963, Maberly et al. 1994). It shows a broad temperature tolerance ranging from 1-26 °C with an optimum at 16-18 °C (Butterwick et al. 2005), is a good competitor for light (Maberly et al. 1994) and ortho-phosphate (SRP), but not for soluble reactive silicate (SRSi) (Van Donk and Kilham 1990). Periods of rapid population increase in *Asterionella* lead to extraction of major nutrients from the surrounding water (Lund 1950). Nutrient depletion, notably of SRSi (Lund et al. 1963) may lead to collapse of

Asterionella blooms (see succession of events in the conceptual PEG model (Sommer et al. 1986)). Alternatively, high levels of chytrid parasitism have been shown to bring *Asterionella* spring blooms rapidly to an end, even before nutrients became limiting for host population growth (Canter and Lund 1948, Van Donk and Ringelberg 1983). Zooplankton grazing is less likely to affect *Asterionella* as it is not easily palatable (Kagami et al. 2004). In summer/autumn, as SRSi levels rise again and irradiation is reduced by deepening of the epilimnion, a second bloom may follow (Lund et al. 1963, Maberly et al. 1994).

The chytrid parasite *Zygorhizidium planktonicum* is a highly virulent, obligate parasite on the diatoms *Asterionella formosa* and *Synedra acus* Kützing (Canter 1953). More than 90% of the host cells in a population may get infected, each infection prohibits host reproduction and quickly kills the host cell (Canter and Lund 1951). As all Chytridiomycota, *Zygorhizidium* is characterized by uniflagellated motile zoospores that actively search for host cells. Zoospores attach to the host cell surface and extract host nutrients via a rhizoid system to support the growth of an epibiontic sporangium. The next generation of zoospores is formed either asexually or sexually and released from the sporangium by dehiscence (Doggett and Porter 1996). Both parasite life stages, zoospores and sporangia, are strongly influenced by their respective environment. During dispersal, the free-swimming zoospores depend entirely on their internal energy stores (Holfeld 2000). They are exposed to predation (Kagami et al. 2007) and water turbulence interfering with their swimming behaviour (Kuhn and Hofmann 1999). Transmission success decreases with decreasing light and ceases completely in dark conditions, probably due to chemotactic localization of hosts through their exuded photosynthetic products (Bruning 1991c, Canter and Jaworski 1981). Once attached, the zoosporangia completely depend on the host cell for sustenance until maturation, hence experiencing both direct and host-mediated environmental influences. The parasite's temperature range for active reproduction is narrower than that of its host. At temperatures below 3 °C the parasite is largely inactive and forms resting spores (Van Donk and Ringelberg 1983) while the upper limit lies just beyond 20 °C (unpublished observations). Sporangia maturation time, number of zoospores per sporangium and zoospore infective lifetime decrease with increasing temperature leading to shorter generation times and lower per capita potential fecundity under warmer conditions (Bruning 1991b). Generally, parasite epidemics are triggered by sufficiently high host abundances as well as temperature and light conditions favourable to transmission (Bruning 1991b).

Here we report temporal host-parasite population dynamics over a depth gradient, including abiotic and biotic variables (light, temperature, pH, ice cover, SRSi, dissolved nitrate (NO_3) and SRP). We present information on timing of host blooms and parasite epidemics, delays in onset of blooms and epidemics across depth and patchiness of host and parasite populations and infection prevalence over the course of the monitored time-period. To our knowledge this is the first study describing simultaneous spatial and temporal variation of host and parasite populations at a moderately fine temporal and spatial resolution.

Methods

Field site and sampling

Water samples for *Asterionella*, chytrid abundances and nutrient chemistry were collected from the centre of Lake Maarsseveen (5°5'8.559"E; 52°8'34.1808"N). The lake covers about 70 ha and has no direct connection with other surface waters (Ringelberg 1981). Ice cover varies from no ice cover in mild winters to several weeks in cold winters. From 24-09-2008 to 21-04-2010 weekly or fortnightly water samples were collected at 0.5, 5, 10, 15 and 20 m depth using a 5 L Uwitec sampler (Uwitec, Mondsee, Austria) and were stored in dedicated polycarbonate containers for transport to the lab. Light, pH and temperature gradients were measured either with a Hydrolab DS5 (Hach, Loveland, USA) when available (21 out of 81 sampling dates) or with a LI-192 Underwater Quantum Sensor (Li Cor, Lincoln, USA) for light measurements, and a portable WTW330i pH meter (WTW, Weilheim, Germany) for pH and temperature measurements. On eight sampling days between 26-08-2009 to 28-09-2009 neither set of equipment was available. Data for global irradiance was obtained from the Royal Netherlands Meteorological Institute KNMI (KNMI 2011).

Analysis of nutrient chemistry, phytoplankton and chytrid abundances

The samples were processed within 4 h after sampling. For SRSi, SRP, NO_3 and dissolved ammonia (NH_4) analysis, subsamples for each depth were filtered over 0.2 µm pore size membrane filters (Whatman, Maidstone, UK) and the filtrate was kept frozen for N and SRP or refrigerated for SRSi analysis according to standard methods (Eaton et al. 2005). Nutrient analysis was executed with a Seal Quaatro autoanalyser 3 (Seal analytical, Mequon, USA) based on Armstrong *et al.* (1967). The detection limits were for SRP = 0.5-3 µg P L^{-1}, for dissolved NO_3 = 2 µg N L^{-1}, for dissolved NH_4 = 7 µg N L^{-1} and SRSi = 0.7 µg Si L^{-1}. For host and chytrid counts, 1 L of each sample was fixed with 8 mL Lugol solution and left

to settle. After one week, the top 900 mL was aspirated off, and the remaining 100 mL was stored in Nalgene polycarbonate bottles for counting.

Counting protocol

A minimum of 200 *Asterionella* cells or 20 fields of view were counted in 1 mL concentrated sample using an inverted microscope (Leica, DMI 4000B, Wetzlar, Germany) according to the Utermöhl method (see (Van Donk and Ringelberg 1983)). All samples were analysed for host and parasite abundance as *Asterionella* cells or *Zygorhizidium* sporangia mL^{-1} and infection prevalence, i.e. percentage of the observed host population infected (Margolis et al. 1982)). Dead *Asterionella* cells carrying dehisced sporangia were counted as infected and may therefore have contributed to an overestimation of infection prevalence.

Definition and calculation of blooms and epidemics

We defined a diatom bloom as a period in which the host abundance rose swiftly and continuously and reached levels that clearly exceeded background levels in the periods preceding and following the bloom (cf. (Maberly et al. 1994)). To establish the onset date of a bloom period, we fitted a logistic growth model to the observed abundance data and defined the onset date as the date at which cell numbers exceeded 30 cells mL^{-1}.

Epidemics are generally defined as spread of infection with $R_0 > 1$ (Anderson and May 1991). High prevalence of infection occurs when the parasite population growth rate surpasses host population growth rate. However, prevalence can yield a skewed impression of parasite impact on host populations if the host population suffer heavy, non-infection related losses. We defined an epidemic (analogous to the definition of a bloom), as the period in which parasite abundances rose swiftly and continuously and reached levels that clearly exceeded background levels in the periods preceding and following the epidemic. The onset date of parasite epidemics was calculated the same way as for the blooms, by fitting a logistic growth model to the observed parasite abundance data and defining the onset date as the date at which chytrid abundance exceeded 30 sporangia mL^{-1}. We also identified a delay in the onset of a bloom or epidemic by depth compared to the onset of a bloom / epidemic at a depth of 5 m, showing a time lag in the onset of the blooms and epidemics progressing down the water column ('depth delay').

Calculation of vertical patchiness

Lloyd's index of patchiness (Lloyd 1967) characterizes the aggregation of individuals in a sample relative to the mean number of individuals present in the sampled neighbourhoods. It is used either as a within-category measure of patchiness ($\hat{I}_P$, based on abundance of host or parasite) or as a cross-category measure of patchiness ($\ddot{I}_{P,XY}$ based on abundance of both, host (X) and parasite (Y)). $\hat{I}_P$ is calculated as

$$\hat{I}_P = 1 + \frac{s^2}{\bar{X}^2} - \frac{1}{\bar{X}}$$

where s^2 is the among-sample variance and $\bar{X}$ the among-sample mean (Hall et al. 2005). When $\hat{I}_P$ equals 1, the distribution of individuals among samples is random; as $\hat{I}_P$ surpasses unity, the distribution of individuals becomes more aggregated, while at $\hat{I}_P$ values below 1, the distribution of individuals is more even than expected in a random (Poisson) distribution (Folt et al. 1993). The cross-category index $\ddot{I}_{P,XY}$ is calculated as

$$\hat{I}_{P,XY} = \frac{\sum_{i=1}^{i=n} X_i Y_i}{\bar{X} \sum_{i=1}^{i=n} Y_i}$$

where X_i and Y_i are abundances of two categories in sample *i* (here host (X) and parasite (Y) abundances) and *n* is the number of samples. The cross-category index works symmetrically and does not change if X and Y are reversed (Hall et al. 2005). Again, an $\ddot{I}_{P,XY}$ value of 1 suggests that individuals of category X and Y are randomly distributed in respect to one other. As aggregations of both categories co-occur, the $\ddot{I}_{P,XY}$ rises above 1, and as aggregations of one category occur in patches where the other category is less abundant, the $\ddot{I}_{P,XY}$ falls below 1 (Folt et al. 1993).

Calculation of Schmidt stability

The Schmidt stability index defines water column stability as the amount of energy (g cm^{-1}) needed to mix the complete water body to a uniform temperature without adding or subtracting any heat (Hutchinson 1957). The index was calculated by the program Lakeanalyzer-2 (Read et al. 2011) using water temperature measurements and data on lake bathymetry. An arbitrary value of 50 g cm^{-1} was chosen to date the onset of stratification.

Statistics

General linear models were used to explore the relationships of the dependent variables host and parasite abundance to independent biotic and abiotic predictors, including abundance of host or parasite (cells or sporangia mL^{-1}), disease prevalence (%), global irradiance (J cm^{-2}), light extinction (m^{-1}), stability (g cm^{-1}), ice cover (none, partial, complete), temperature (°C), pH, SRSi (µmol Si L^{-1}) and NO_3 (µmol N L^{-1}) for each depth 5, 10 and 15 m separately (using the lm function in R package stats (R 2011)). Missing values were interpolated by splining (function na.spline in R package zoo). Estimates for the missing temperature and pH data points were interpolated by fitting a sine function to the temperature and pH data series, evaluated with least squares goodness of fit . General linear model selection was conducted by standard AIC methods, starting from the full model including all predictors and stepwise deleting the least significant predictor (stepAIC function in R package MASS). The residuals of the resulting models were tested for presence of autocorrelation by using the autocorrelation function (acf) and partial autocorrelation function (pacf) of the R package stats. If significant autocorrelation was present in the residuals, an autoregressive model (ARMA) was fitted to explore the order of the autoregression and the moving average (arma in R package tseries). Subsequently, this ARMA model was fitted to both sides of the original model to correct for the error structure. The residuals of this model fit were then again checked for absence of autocorrelation.

Population growth rates of host and parasite were calculated by fitting exponential growth models to their abundance data. Model fits were obtained by minimization of the residual sum of squares of observed and modelled values. These growth models were used to calculate the starting date of blooms and epidemics, i.e. the day when abundance exceeded 30 cells or sporangia mL^{-1}. Abundance data for host and parasite were log+1 transformed for plotting Fig. 3. Statistical analysis and plot graphing were carried out in R (R 2011), Statistica 8.0 (StatSoft GmbH, Hamburg, Germany) and SigmaPlot 11.0 (Systat Software Inc., San Jose, USA).

Results

Temperature, light and pH

Temperature at each depth showed seasonal and depth-related courses and ranged from 1.6 to 21.1 °C. Two short bouts of ice cover were observed with either partial or full ice cover from 5-01-2009 to 21-01-2009 and 13-01-2010 to 10-03-2010. Thermal stratification (based on a Schmidt stability value > 50 g cm^{-1}) started both years in early April and broke down in late November. In autumn and winter isothermal conditions prevailed with the exception of two short periods of inverted stratification under

ice (Fig. 1a,b). During stratified conditions the thermocline was located at around 8 m. Light extinction coefficient (m^{-1}) time courses showed no seasonal pattern in Lake Maarsseveen with an average of 0.77 (range: 0.37- 1.3, SD= 0.23) which translated into an average photic zone depth of 6.7 m (range: 3.55-12.58 m, SD=1.98 m). The depth of the photic zone was defined by the 1% limit of incoming irradiation, given the actual light extinction coefficient. pH values in the lake ranged from 7.07 to 8.56. Generally pH decreased with depth and towards the end of the phytoplankton growing season.

Nutrients

SRSi ranged from 14 to 89 µmol Si L^{-1} with a mean value of around 65 µmol Si L^{-1} across all depths during isothermal conditions. With onset of thermal stratification, SRSi concentrations in the epilimnion started to decrease probably due to uptake by diatoms. At the same time, concentrations gradually increased in the hypolimnion probably due to remineralisation of diatom shells. Nitrate showed a comparable time course per depth, with values ranging from the detection limit to 40 µmol N L^{-1} (Fig. 2a,b). SRP and NH_4 were mostly below the detection limit (data not shown).

Host abundance

During a period of two winters and one summer, four *Asterionella* blooms were observed. The seasonal cycle showed a low pelagic pre-bloom population which increased in late winter to early spring to form typical *Asterionella* spring blooms in early 2009 (further called bloom 1) and in early 2010 (further called bloom 4). Also a summer (bloom 2) and an autumn bloom (bloom 3) were observed in 2009. All peak abundances and the dates of onset and peak of bloom are shown in Table 1. All four blooms occurred across all depths, but not always with a uniform onset date or abundance distribution across depths (Fig. 3a).

Parasite abundance and infection prevalence

During the same time period, two typical spring epidemics in early 2009 (epidemic 1) and early 2010 (epidemic 4) were observed. Additionally, a very marginal epidemic in summer 2009 (epidemic 2) and an autumn 2009 epidemic (epidemic 3) were observed. Each epidemic was preceded by a host bloom. The observed spring epidemics showed high sporangia abundances and infection prevalence. The epidemics observed in summer/autumn were either low in sporangia abundance and infection prevalence, as in epidemic 2 or high in sporangia abundance but low in infection prevalence, as in epidemic 3. Again, all

prevalence, sporangia peak abundance and dates of onset and peak of epidemic are shown in Table 1. Prevalence of infection is a measure of the percentage of host population that is infected and is therefore a measure of parasite impact on the host population rather than a measure of parasite abundance. Prevalence peaked after the parasite peak abundance when host numbers were already declining due to infection losses. In summer, sporadic high prevalence samples reflected rather an occasional infection at very low host abundance than sustained elevated parasite abundances (Fig. 3b,c).

Environmental signals in host and parasite abundance time courses

Host abundance (cells mL^{-1}) was related to both biotic and abiotic predictors whose importance changed with depth. Host abundance showed a significant, positive relationship with sporangia abundance at all depths. Within the upper 10 m, environmental predictors such as SRSi, temperature, Schmidt stability and global irradiance showed a significant relationship with host abundance, but were completely absent at 15 m. The model fits increased with depth (Table 2).

Parasite abundance (sporangia mL^{-1}) showed a significant, positive relationship with host abundance and with infection prevalence across all depths. In the upper 10 m, environmental predictors, notably temperature, light extinction and global irradiance showed a significant relationship with parasite abundance, but were completely absent at 15 m. Again, the model fit increased with depth (Table 2).

Depth delay

Production of both host and parasite seemed to occur within the uppermost 5 m during stratified as well as isothermal conditions. The onset date was generally time-lagged with depth: for blooms: delay of onset = $e^{0.134\,(depth)}$, R^2_{adj} = 0.5665, P = <0.0001, and epidemics: delay of onset = $e^{0.137\,(depth)}$-10, R^2_{adj} = 0.262, P = <0.0001 (Fig. 4a,b).

Seasonal vertical patchiness

The vertical distribution of host abundance showed seasonal and disease-related signals. During stratified periods, the host population aggregated more in the production layer and therefore showed higher $\hat{I}_P$ values. However, isothermal mixing and parasite epidemics seemed to induce a more random host population distribution with $\hat{I}_P$ values moving closer to unity (Fig. 5a). Vertical distribution of parasite abundance indicated that the parasite occurred in patches ($\hat{I}_P$ >1) during most of the year, but

was more randomly distributed across depths during epidemics ($\hat{I}_P \approx 1$ (Fig. 5b)). Parasites responded favourably to host density, as the cross-category patchiness index for host and parasite abundances (Fig. 5c) indicated that higher abundance patches of parasites co-occurred with higher abundance patches of hosts for most of the year ($\hat{I}_{P,XY} > 1$). Again, during isothermal mixing but also during the high prevalence spring epidemics, this association became weaker and the populations were more randomly distributed in respect to each other. Summer and autumn blooms and epidemics (2 and 3) did not show a randomizing effect on the host-parasite association ($\hat{I}_{P,XY}$ values remained above 1).

Discussion

Host-parasite population dynamics and disease impact showed clear seasonal signals with two typical *Asterionella* spring blooms followed by high prevalence chytrid epidemics and two summer/autumn blooms followed by lower parasite prevalence epidemics. Host and parasite abundances showed significant relationships with biotic (parasite or host abundance) and abiotic (SRSi, light, temperature and Schmidt stability) predictors in the upper 10 m but only with biotic predictors at 15 m. Blooms and epidemics both started in the upper water layers well within the photic zone and subsequently sank to deeper layers. Host and parasite vertical distribution showed both seasonal and ecological signatures. Vertical patchiness of the host was disrupted by entrainment during the isothermal mixing period and reduced during parasite epidemics.

Host and parasite abundances

The onset of *Asterionella* spring blooms was likely triggered by improving but still low light conditions (Maberly et al. 1994), as *Asterionella* is a good competitor for light. A pelagic population of *Asterionella* was present year-round so that the spring host population development might have started from an overwintering pelagic inoculum. However, the role of colonies re-suspending from the sediment is largely unknown, but large-scale resuspension of *Asterionella* colonies has neither been observed in Lake Maarsseveen (reversed sedimentation traps; data not shown) nor elsewhere (Lund 1949). Host abundance showed a significantly positive relationship with parasite abundance across all depths and a significantly negative relationship with prevalence of infection at 10 m. Generally, parasite abundance increased with host abundance but prevalence of infection peaked when host numbers were already declining due to disease-related losses. Within the upper 10 m, host abundance also showed significant relationships with abiotic predictors. SRSi decreased as host abundance increased, suggesting that

Asterionella reduced SRSi levels by uptake. However, the highest abundance host bloom occurred in autumn 2009 when pre-bloom SRSi levels were already lower than the SRSi levels at the end of spring blooms, suggesting that SRSi levels were not limiting in Lake Maarsseveen. The rather sudden end of spring blooms is more likely have been brought about by heavy parasitism well before competitive exclusion due to SRSi limitation could become important (see (Van Donk and Ringelberg 1983)). Thereby parasitism could potentially uncouple phytoplankton succession from nutrient limitation-mediated competitive exclusion (Canter and Lund 1951). Light availability (global irradiance) showed a significantly positive effect on host abundance at 10 m, suggesting that light conditions were sufficient at 5 m but limiting at 10 m. Also Schmidt stability had a significantly negative effect at 10 m only. During stratified conditions, the thermocline was located at around 8 m depth, thus the population sampled at 10 m was just below the thermocline and therefore not always entrained in the epilimnion. At 15 m, host population increase was most probably not a result of population reproduction within the hypolimnion but of the population sinking towards the sediment, whereby moribound and dead cells (hence also infected cells) are known to sink more readily through the thermocline (Lund et al. 1963). The sinking of parasitized dying cells together with the dampened environmental variation at 15 m may explain why host abundance showed a relationship with parasite abundance only and why the fit of the model increased with depth.

Chytrid epidemics were likely triggered by both sufficient host densities and favourable environmental conditions for parasite activity and transmission. Parasite abundance was positively related to host abundance as shown also in Ibelings *et al.* (2011). Generally, the parasite needs a minimum host density to reproduce above replacement rate (Bruning 1991b). It profits from increasing host densities, probably due to decreased host-searching time and increased host encounter rates for zoospores. However, host density was not the only factor driving parasite population growth. At 5 m, parasite abundance showed a significantly negative relationship with light extinction, suggesting the importance of sufficiently high light conditions for transmission. As zoospores locate the host through chemotaxis to its photosynthetic exudates, transmission success decreases with decreasing light and ceases completely in darkness (Bruning 1991c). At 5 and 10 m, parasite abundance showed a significantly negative relationship with temperature, suggesting that warmer temperatures in summer reduced parasite abundance. Many lifecycle traits such as sporangia maturation time, zoospore infective lifetime and the number of zoospore per sporangium decrease with increasing temperatures (Bruning 1991b), hence very warm temperatures may hamper reproductive success. The temperature range for parasite activity was generally narrower than that of its host which may be an insurance strategy of the

parasite to time its activity more securely within the time of its host's activity. At 15 m parasite abundance was related to host abundance only, which may be explained by the sinking of parasitized host cells and the relatively stable environment in the hypolimnion.

The blooms and epidemics observed in spring and summer differed in size and disease impact. The two spring blooms fitted into the general patterns described in Ibelings *et al.* (2011) on how the impact of spring epidemics depended on winter conditions and timing of events: In cold winters when water temperatures fell below 3 °C the host population started to grow while the parasite was still inactive. With rising spring temperatures, the parasite became active and encountered a sufficient host density for successful epidemic development (Ibelings et al. 2011). But if the host bloom occurred under ice, the parasite might not be able to profit from it at all, see early bloom 1, (Fig. 3a). In warmer winters, when the water temperature remained above 3 °C, the host population actually grew faster, but was parasitized all the time, resulting in a lower and delayed host peak abundance, lower parasite peak abundance and lower peak infection prevalence (Ibelings et al. 2011). The blooms observed in summer/autumn developed faster than the spring blooms and were quickly followed by lower prevalence epidemics that were not able to regulate host populations to the same extent as during spring epidemics. Several reasons might explain the lower parasite success despite high host densities in summer. Successful parasite invasion and maintenance may have been hampered by decreased transmission success due to warmer temperatures. Higher abundance of potential zoospore predators, like *Daphnia* (Kagami et al. 2007) or protection of the *Asterionella* population by its epibiont *Salpingoeca sp. (*which has already been shown to be an efficient bacterivore (Simek et al. 2004)) at the time of bloom 3 might also explain the lower disease impact. And finally, summer/autumn *Asterionella* populations may live under generally more nutrient-poor conditions. Nutrient availability affects not only host population growth rate but also its cellular elemental composition (Sterner 2002). Such host-mediated effects of resource availability were shown to influence parasite reproduction success (Hall et al. 2009). In the *Asterionella*-chytrid system, phosphorus limitation of the host lead to decreased zoospore production per sporangium (Bruning 1991a). Complex effects of host-mediated resource availability on parasite production and epidemic development of disease were explored in a mathematical model (Gerla et al. (submitted)), showing how parasite R_0 increased with dissolved nutrient concentration through increased parasite reproduction on hosts. Under certain conditions however, chaotic host-parasite cycles were observed whose amplitudes increased with nutrient enrichment, leading to the collapse of the parasite population.

Vertical population structuring

Patchy distribution of organisms likely influences interaction rates between con- and heterospecifics, thereby affecting population and community processes (Folt et al. 1993). Traditionally, formation of patches was considered purely a product of physical factors (Abraham 1998). But also ecological drivers influence patch formation: exploitative competition, predation and parasitism all interact with the physical environment and their intricate interplay varies seasonally and geographically (Reid et al. 1990). As the chytrid depends on both host availability and light conditions, the vertical distribution (patchiness) of the host population may be crucial for parasite invasion and persistence (Keeling 1999). Host vertical abundance distribution showed a varied picture with higher $\hat{I}_P$ values between bloom periods and lower values during blooms, parasite epidemics and isothermal mixing periods. Host production was in the upper, photic water layers but during isothermal conditions the mixing of the water column spread the *Asterionella* population nearly randomly across depths. Ice cover and the resulting inverted stratification led to some vertical structuring, as the *Asterionella* population stayed closer to where it was produced. Higher $\hat{I}_P$ host values during the thermally stratified period showed the effects of entrainment of the *Asterionella* population within the epilimnion. However, during calm weather, part of the population was sinking. Interestingly, in times of parasite epidemics host patchiness seemed to be reduced as well. This may have been a combined effect of higher host abundances and more favourable light conditions for the infection process in the epilimnion.

For most of the year, the vertical distribution of parasite abundance was fairly patchy (high $\hat{I}_P$ prevalence values), the disease was rare and occurred only in segregated pockets. With onset of spring epidemics (epidemics 1 and 4), the parasite spread across the water column quickly and its patchiness was reduced. At the start of summer epidemics (epidemics 2 and 3) the patchiness of parasite abundance was not reduced to the same level as in spring epidemics. In the cross category patchiness index, higher $\hat{I}_{P,XY}$ values indicated that higher abundance patches of the parasite co-occurred with higher abundance patches of the host during thermally stratified conditions and in absence of epidemics, when pockets of the parasite were dependent on sufficiently dense pockets of *Asterionella*. However, during isothermal conditions the $\hat{I}_{P,XY}$ values came closer to unity indicating that host and parasite aggregations were more randomly distributed in respect to one other. This suggests that the parasite distribution was not driven entirely by host density in isothermal conditions but also depended on environmental factors. Similarly, the $\hat{I}_{P,XY}$ values were near 1 during the summer/autumn epidemics which might reflect the impact of the parasite on the host population patch densities.

Seasonal climatic and physical variability influence parasite abundance and transmission through environmentally driven changes in host density but also through environmentally driven changes in the host-parasite interaction (Johnson et al. 2009). Vertical gradients in abiotic factors and in patchiness of host and parasite populations expose host and parasite individuals to different environmental conditions even within a single population. As a consequence, this also leads to differences in disease exposure and infection risks along such environmental gradients (Wolinska et al. 2011). Changes in environmental conditions affect host abundance and host nutritional status which, in turn, influence parasite per capita reproductive output and transmission rates (Gerla et al. (submitted), Johnson et al. 2007). Environmental variation can also affect overall disease impact and severity (Paull and Johnson 2011) and modulate the outcome of specific host genotype by parasite genotype interactions (Schoebel et al. 2011, Wolinska and King 2009), resulting in changes in the strength and direction of parasite-mediated clonal host selection.

Our study confirmed that host and parasite populations occur in a temporally and spatially variable environment and show considerable vertical population structuring. Environmental factors such as seasonal variation in light and temperature, but also depth-related light and chemical gradients lead to temporally and spatially structured populations. Vertical positioning and patchiness of the host population can have profound effects on parasite reproductive success which is shaped by both host density but also by environmental conditions. This report on spatio-temporal distributions of host and parasite populations in Lake Maarsseveen aims at contributing to the general insight needed into the complex interplay between abiotic and biotic drivers and how these affect the course and outcome of host-parasite interactions.

Acknowledgments

We want to thank our colleagues Koos Swart, Andrea Koopmans, Maciej Bartosiewicz and Anna Przytulska-Bartosiewicz for field sampling support, Wolf Mooij for data interpolation advice and two anonymous reviewers for improving this manuscript. ASG is supported by grant 816.01.018 of the Dutch Organization for Scientific Research - Earth and Life Science Foundation (NWO-ALW) to BWI and EvD. LdSD is supported by grant 817.01.007 of NWO-ALW. A part of the data presented here was already included in an earlier publication (Ibelings et al. 2011). This is NIOO-KNAW publication number 5160.

References

Abraham E. R. (1998) The generation of plankton patchiness by turbulent stirring. *Nature,* **391**, 577-580.

Altizer S., Dobson A., Hosseini P., Hudson P., Pascual M. & Rohani P. (2006) Seasonality and the dynamics of infectious diseases. *Ecology Letters,* **9**, 467-484.

Anderson R. M. & May R. M. (1991) *Infectious Diseases of Humans: Dynamics and Control*. Oxford: Oxford University Press.

Armstrong F. A. J., Stearns C. R. & Strickland J. D. H. (1967) Measurement of upwelling and subsequent biological processes by means of Technicon Autoanalyzer and associated equipment. *Deep-Sea Research,* **14**, 381-389.

Arneberg P., Skorping A., Grenfell B. & Read A. F. (1998) Host densities as determinants of abundance in parasite communities. *Proceedings of the Royal Society of London Series B-Biological Sciences,* **265**, 1283-1289.

Bruning K. (1991a) Effects of phosphorus limitation on the epidemiology of a chytrid phytoplankton parasite. *Freshwater Biology,* **25**, 409-417.

Bruning K. (1991b) Effects of temperature and light on the population-dynamics of the *Asterionella-Rhizophydium* association. *Journal of Plankton Research,* **13**, 707-719.

Bruning K. (1991c) Infection of the diatom *Asterionella* by a chytrid. 1. Effects of light on reproduction and infectivity of the parasite. *Journal of Plankton Research,* **13**, 103-117.

Butterwick C., Heaney S. I. & Talling J. F. (2005) Diversity in the influence of temperature on the growth rates of freshwater algae, and its ecological relevance. *Freshwater Biology,* **50**, 291-300.

Canter H. M. & Jaworski G. H. M. (1981) The effect of light and darkness upon infection of *Asterionella formosa* Hassall by the chytrid *Rhizophydium planktonicum* Canter emend. *Annals of Botany,* **47**, 13-30.

Canter H. M. & Lund J. W. G. (1948) Studies on plankton parasites. I. Fluctuations in the numbers of *Asterionella formosa* Hassal in relation to fungal epidemics. *New Phytologist,* **47**, 238-261.

Canter H. M. & Lund J. W. G. (1951) Studies on plankton parasites. III. Examples of the interaction between parasitism and other factors determining the growth of diatoms. *Annals of Botany,* **15**, 359-371.

Canter H. M., & Lund , J.W.G. (1953) Studies on plankton parasites. II. The parasitism of diatoms with special reference to lakes in the English lake district. *Transactions of the British Mycological Society,* **36**, 13-37.

Dangerfield C. E., Ross J. V. & Keeling M. J. (2009) Integrating stochasticity and network structure into an epidemic model. *Journal of the Royal Society Interface,* **6**, 761-774.

Doggett M. S. & Porter D. (1996) Sexual reproduction in the fungal parasite, *Zygorhizidium planktonicum*. *Mycologia,* **88**, 720-732.

Eaton A. D., Clesceri L. S., Rice E. W., Greenberg A. E. & Franson M. A. H. (Eds) (2005) *Standard Methods for the Examination of Water & Wastewater*. Washington: American Public Health Association.

Ebert D., Zschokke-Rohringer C. D. & Carius H. J. (2000) Dose effects and density-dependent regulation of two microparasites of *Daphnia magna*. *Oecologia,* **122**, 200-209.

Folt C., Schulze P. C. & Baumgartner K. (1993) Characterizing a zooplankton neighborhood - small-scale patterns of association and abundance. *Freshwater Biology,* **30**, 289-300.

Frost P. C., Ebert D. & Smith V. H. (2008) Responses of a bacterial pathogen to phosphorus limitation of its aquatic invertebrate host. *Ecology,* **89**, 313-318.

Gerber L. R., McCallum H., Lafferty K. D., Sabo J. L. & Dobson A. (2005) Exposing extinction risk analysis to pathogens: Is disease just another form of density dependence? *Ecological Applications,* **15**, 1402-1414.

Gerla D. J., Gsell A. S., Kooi B. W., Ibelings B. W., van Donk E. & Mooi j. W. M. ((xxxx)) Alternative states and population crashes in a resource-susceptible-infected model for planktonic parasites and hosts. *Freshwater Biology*, xx, xxx-xxx.

Hall S. R., Duffy M. A., Tessier A. J. & Caceres C. E. (2005) Spatial heterogeneity of daphniid parasitism within lakes. *Oecologia,* **143**, 635-644.

Hall S. R., Knight C. J., Becker C. R., Duffy M. A., Tessier A. J. & Caceres C. E. (2009) Quality matters: resource quality for hosts and the timing of epidemics. *Ecology Letters,* **12**, 118-128.

Holfeld H. (2000) Relative abundance, rate of increase, and fungal infections of freshwater phytoplankton. *Journal of Plankton Research,* **22**, 987-995.

Hutchinson G. (1957) *A Treatise on Limnology, vol. 1, Geography, Physics, and Chemistry*, 1015 pp: New York: Wiley.

Ibelings B. W., De Bruin A., Kagami M., Rijkeboer M., Brehm M. & van Donk E. (2004) Host parasite interactions between freshwater phytoplankton and chytrid fungi (Chytridiomycota). *Journal of Phycology,* **40**, 437-453.

Ibelings B. W., Gsell A. S., Mooij W. M., Van Donk E., Van Den Wyngaert S. & de Senerpont Domis L. N. (2011) Chytrid infections and diatom spring blooms: paradoxical effects of climate warming on fungal epidemics in lakes. *Freshwater Biology,* **56**, 754-766.

Johnson P. T. J., Chase J. M., Dosch K. L., Hartson R. B., Gross J. A., Larson D. J., Sutherland D. R. & Carpenter S. R. (2007) Aquatic eutrophication promotes pathogenic infection in amphibians. *Proceedings of the National Academy of Sciences of the United States of America,* **104**, 15781-15786.

Johnson P. T. J., Ives A. R., Lathrop R. C. & Carpenter S. R. (2009) Long-term disease dynamics in lakes: causes and consequences of chytrid infections in *Daphnia* populations. *Ecology,* **90**, 132-144.

Kagami M., Ibelings B. W., de Bruin A. & Van Donk E. (2004) Vulnerability of *Asterionella formosa* to *Daphnia* grazing: impact of a fungal parasite (ed. J. Jones), pp. 350-354. Lahti, Finland.

Kagami M., von Elert E., Ibelings B. W., de Bruin A. & Van Donk E. (2007) The parasitic chytrid, *Zygorhizidium*, facilitates the growth of the cladoceran zooplankter, *Daphnia*, in cultures of the inedible alga, *Asterionella*. *Proceedings of the Royal Society B-Biological Sciences,* **274**, 1561-1566.

Keeling M. J. (1999) The effects of local spatial structure on epidemiological invasions. *Proceedings of the Royal Society of London Series B-Biological Sciences,* **266**, 859-867.

Keeling M. J. & Eames K. T. D. (2005) Networks and epidemic models. *Journal of the Royal Society Interface,* **2**, 295-307.

Keeling M. J. & Grenfell B. T. (2000) Individual-based perspectives on R-0. *Journal of Theoretical Biology,* **203**, 51-61.

KNMI. (2011) Klimatologie. Available at: http://www.knmi.nl/klimatologie/index.html.

Krasnov B. R., Mouillot D., Shenbrot G. I., Khokhlova I. S. & Poulin R. (2010) Deconstructing spatial patterns in species composition of ectoparasite communities: the relative contribution of host composition, environmental variables and geography. *Global Ecology and Biogeography,* **19**, 515-526.

Kuhn S. F. & Hofmann M. (1999) Infection of *Coscinodiscus granii* by the parasitoid nanoflagellate *Pirsonia diadema*: III. Effects of turbulence on the incidence of infection. *Journal of Plankton Research,* **21**, 2323-2340.

Laine A. L. (2007) Pathogen fitness components and genotypes differ in their sensitivity to nutrient and temperature variation in a wild plant-pathogen association. *Journal of Evolutionary Biology,* **20**, 2371-2378.

Lloyd M. (1967) `Mean Crowding'. *Journal of Animal Ecology,* **36**, 1-30.

Lund J. W. G. (1949) Studies on *Asterionella*. 1. The origin and nature of the cells producing seasonal maxima. *Journal of Ecology,* **37**, 389 - 419.

Lund J. W. G. (1950) Studies on *Asterionella*. 2. Nutrient depletion and the spring maximum. *Journal of Ecology,* **38**, 1 - 35.

Lund J. W. G., Mortimer C. H. & Mackereth F. J. (1963) Changes in depth and time of certain chemical and physical conditions and of standing crop of *Asterionella formosa* Hass in the North Basin of Windermere in 1947. *Philosophical Transactions of the Royal Society of London Series B-Biological Sciences,* **246**, 255-290.

Maberly S. C., Hurley M. A., Butterwick C., Corry J. E., Heaney S. I., Irish A. E., Jaworski G. H. M., Lund J. W. G., Reynolds C. S. & Roscoe J. V. (1994) The rise and fall of *Asterionella formosa* in the south basin of Windermere - analysis of a 45-year series of data. *Freshwater Biology,* **31**, 19-34.

Margolis L., Esch G. W., Holmes J. C., Kuris A. M. & Schad G. A. (1982) The use of ecological terms in parasitology (report of an ad hoc committee of the American-Society of Parasitologists). *Journal of Parasitology,* **68**, 131-133.

Mitchell S. E., Rogers E. S., Little T. J. & Read A. F. (2005) Host-parasite and genotype-by-environment interactions: Temperature modifies potential for selection by a sterilizing pathogen. *Evolution,* **59**, 70-80.

Paull S. H. & Johnson P. T. J. (2011) High temperature enhances host pathology in a snail-trematode system: possible consequences of climate change for the emergence of disease. *Freshwater Biology,* **56**, 767-778.

R Development Core Team (2011) *R: A Language and Environment for Statistical Computing*. Vienna: R Development Core Team, R Foundation for Statistical Computing.

Read J. S., Hamilton D. P., Jones I. D., Muraoka K., Winslow L. A., Kroiss R., Wu C. H. & Gaiser E. (2011) Derivation of lake mixing and stratification indices from high-resolution lake buoy data. *Environmental Modelling and Software,* **26**, 1325-1336.

Reid P. C., Lancelot C., Gieskes W. W. C., Hagmeier E. & Weichart G. (1990) Phytoplankton of the North Sea and its dynamics - a review. *Netherlands Journal of Sea Research,* **26**, 295-331.

Ringelberg J. (1981) Introduction to the research area. *Hydrobiological Bulletin,* **15**, 5-9.

Schoebel C. N., Tellenbach C., Spaak P. & Wolinska J. (2011) Temperature effects on parasite prevalence in a natural hybrid complex. *Biology Letters,* **7**, 108-111.

Simek K., Jezbera J., Hornak K., Vrba J. & Sed'a J. (2004) Role of diatom-attached choanoflagellates of the genus *Salpingoeca* as pelagic bacterivores. *Aquatic Microbial Ecology,* **36**, 257-269.

Sommer U., Gliwicz Z. M., Lampert W. & Duncan A. (1986) The PEG-model of seasonal succession of planktonic events in fresh waters. *Archiv für Hydrobiologie,* **106**, 433-471.

Sterner R. W., Elser, J.J. (2002) *Ecological Stoichiometry: The Biology of Elements from Molecules to the Biosphere*. Princeton: Princeton University Press.

Van Donk E. & Kilham S. S. (1990) Temperature effects on silicon-limited and phosphorus-limited growth and competitive interactions among 3 diatoms. *Journal of Phycology,* **26**, 40-50.

Van Donk E. & Ringelberg J. (1983) The effect of fungal parasitism in the succession of diatoms in Lake Maarsseveen 1 (The Netherlands). *Freshwater Biology,* **13**, 241-251.

Wolinska J. & King K. C. (2009) Environment can alter selection in host-parasite interactions. *Trends in Parasitology,* **25**, 236-244.

Wolinska J., Seda J., Koerner H., Smilauer P. & Petrusek A. (2011) Spatial variation of *Daphnia* parasite load within individual water bodies. *Journal of Plankton Research,* **33**, 1284-1294.

Legends

Table 1

Onset and peak abundance dates, the peak abundance (cells or sporangia mL^{-1}) and peak prevalence (%) by depth. Additionally, the 'depth delay' of onset of the bloom and the delay from onset of the bloom to onset of the epidemic are shown.

Table 2

Results of the general linear models on the arma-transformed data series for the dependent variables host abundance and parasite abundance at depths 5, 10 and 15 m. The numbers in brackets of the arma model indicate the autoregressive order and the order of the moving average respectively.

Fig. 1

Temperature (°C) contour plot for the whole monitoring period with linear integration between measured depths (upper panel a), and global irradiance (J cm^{-2}) and Schmidt stability (g cm^{-1}) dynamics for the same period (lower panel b). The cutoff value of 50 g cm^{-1} for onset and end of thermal stratification periods is indicated with a dashed line. Periods of partial and full ice cover (grey), blooms (dark grey) and epidemics (black) are indicated, while the four blooms are indicated with numbers above panel a.

Fig. 2

SRSi (µmol Si L^{-1}; upper panel a) and dissolved NO_3 (µmol N L^{-1}; lower panel b) dynamics over the monitored time period with linear integration between measured depths. The four host blooms are indicated with white numbers on panel a.

Fig. 3

Host abundance (log+1 cells mL^{-1}; upper panel a), parasite abundance (log+1 sporangia mL^{-1}; middle panel b) and infection prevalence (% of host individuals infected; lower panel c) are presented with linear integration between measured depths. Abundance data were log+1 transformed to improve visibility. Four host blooms (indicated with white numbers on panel a) and four epidemics are visible (white numbers on panel b). Periods of ice cover are indicated with a white line in panel b.

Fig. 4

Depth delay in days for the delay in onset dates compared to the onset date of the same event at a depth of 5 m. Blooms (upper panel a): delay onset of the bloom to onset of the same bloom at a depth

of 5 m = $e^{(0.137*depth)}$, R^2_{adj} = 0.5665, *P* = <0.0001; and epidemics (lower panel b): delay onset of the epidemic to onset of the same epidemic at a depth of 5 m = $e^{(0.134*depth)}$ - 10, R^2_{adj} = 0.262, *P* = <0.0001. Onset date for depth 0.5 m was available only for bloom/epidemic 4.

Fig. 5

Temporal changes in Lloyd's index of patchiness for vertical host abundance (upper panel a), parasite abundance (middle panel b) and host and parasite aggregation co-occurrence (lower panel c) with indications of time periods of isothermal conditions (grey, solid) and inverted stratification (grey, dotted), of bloom (dark grey) and epidemic (black) periods as well as of partial and full ice cover (light grey).

Table 1

bloom	*depth (m)*	*host bloom onset date*	*host bloom peak date*	*host peak abundance*	*depth delay onset bloom (days)*	*parasite epidemic onset date*	*parasite abundance peak date*	*parasite peak abundance*	*peak prevalence*	*delay onset bloom to onset epidemic (days)*
1	5	28-12-2008	2-3-2009	530	0	15-2-2009	2-3-2009	405	77	49
1	10	30-12-2008	2-3-2009	640	2	14-2-2009	2-3-2009	454	71	46
1	15	29-12-2008	2-3-2009	444	1	17-2-2009	2-3-2009	230	52	50
1	20	12-1-2009	2-3-2009	633	15	16-2-2009	2-3-2009	370	58	35
2	5	26-5-2009	10-6-2009	305	0	10-6-2009	10-6-2009	15	6	15
2	10	27-5-2009	17-6-2009	207	1	3-6-2009	3-6-2009	9	8	7
2	15	5-6-2009	10-6-2009	174	10	10-6-2009	10-6-2009	5	9	5
2	20	8-6-2009	10-6-2009	261	13	na	na	0	0	na
3	5	27-9-2009	21-10-2009	2032	0	15-10-2009	28-10-2009	288	22	18
3	10	27-9-2009	28-10-2009	2106	0	11-10-2009	28-10-2009	446	21	14
3	15	11-10-2009	21-10-2009	820	14	23-10-2009	28-10-2009	119	23	12
3	20	21-10-2009	3-11-2009	289	24	29-10-2009	3-11-2009	21	14	8
4	0.5	20-2-2010	24-3-2010	307	-6	18-3-2010	24-3-2010	84	82	26
4	5	26-2-2010	6-4-2010	264	0	28-3-2010	6-4-2010	65	80	30
4	10	2-3-2010	6-4-2010	264	4	19-3-2010	6-4-2010	81	82	17
4	15	19-2-2010	6-4-2010	286	-7	29-3-2010	6-4-2010	191	80	38
4	20	10-3-2010	6-4-2010	314	12	26-3-2010	6-4-2010	72	96	16

Table 2

			coefficient	*coefficient standard error*	*t-value*	*P*
parasite	*5 m*	R^2_{adj} = 0.48, arma(1,2), $F_{6,74}$ = 13.3, P <0.0001				
	intercept		144.70	56.29	2.57	**0.012**
	SiO_2		-1.29	0.61	-2.12	**0.037**
	host		0.05	0.02	2.90	**0.005**
	prevalence		2.36	0.37	6.43	**< 0.001**
	light extinction		-59.65	28.52	-2.09	**0.040**
	ice cover		-12.56	8.84	-1.42	0.160
	temperature		-4.06	1.62	-2.50	**0.015**
	10 m	R^2_{adj} = 0.69, arma(1,1), $F_{7,79}$ = 26.6, P <0.0001				
	intercept		-295.40	210.53	-1.40	0.165
	SiO_2		0.46	0.35	1.30	0.196
	host		0.12	0.01	9.88	**< 0.001**
	prevalence		1.40	0.25	5.51	**< 0.001**
	stability		0.07	0.03	2.44	**0.017**
	global irradiance		-0.02	0.01	-2.33	**0.023**
	temperature		-2.70	1.32	-2.05	**0.045**
	pH		37.56	26.46	1.42	0.160
	15 m	R^2_{adj} = 0.71, no arma, $F_{2,80}$ = 100.4, P <0.0001				
	intercept		-4.94	2.34	-2.11	**0.038**
	host		0.19	0.02	11.64	**< 0.001**
	prevalence		0.43	0.13	3.28	**0.002**
host	*5 m*	R^2_{adj} = 0.15, arma(0,2), $F_{5,75}$ = 3.9, P =0.003				
	intercept		-875.87	1504.41	-0.58	0.562
	SiO_2		-10.69	4.51	-2.37	**0.020**
	sporangia		1.75	0.52	3.39	**0.001**
	stability		-0.72	0.42	-1.72	0.089
	temperature		-2.29	12.72	-0.18	0.858
	pH		202.80	203.59	1.00	0.322
	10 m	R^2_{adj} = 0.59, arma(3,2), $F_{8,71}$ = 14.9, P <0.0001				
	intercept		3483.66	1692.83	2.06	**0.043**
	SiO_2		-7.37	4.16	-1.77	0.080
	NO_3		-5.61	7.11	-0.79	0.432
	sporangia		4.77	0.58	8.26	**< 0.001**
	prevalence		-5.31	2.18	-2.44	**0.017**
	irradiance		0.18	0.09	2.06	**0.043**
	stability		-0.82	0.30	-2.75	**0.008**
	temperature		15.27	11.11	1.38	0.170
	pH		-387.19	215.44	-1.80	0.077
	15 m	R^2_{adj} = 0.63, arma(3,0), $F_{1,78}$ = 134.6, P <0.0001				
	intercept		31.74	6.62	4.79	**< 0.001**
	sporangia		3.45	0.30	11.60	**< 0.001**

Figures

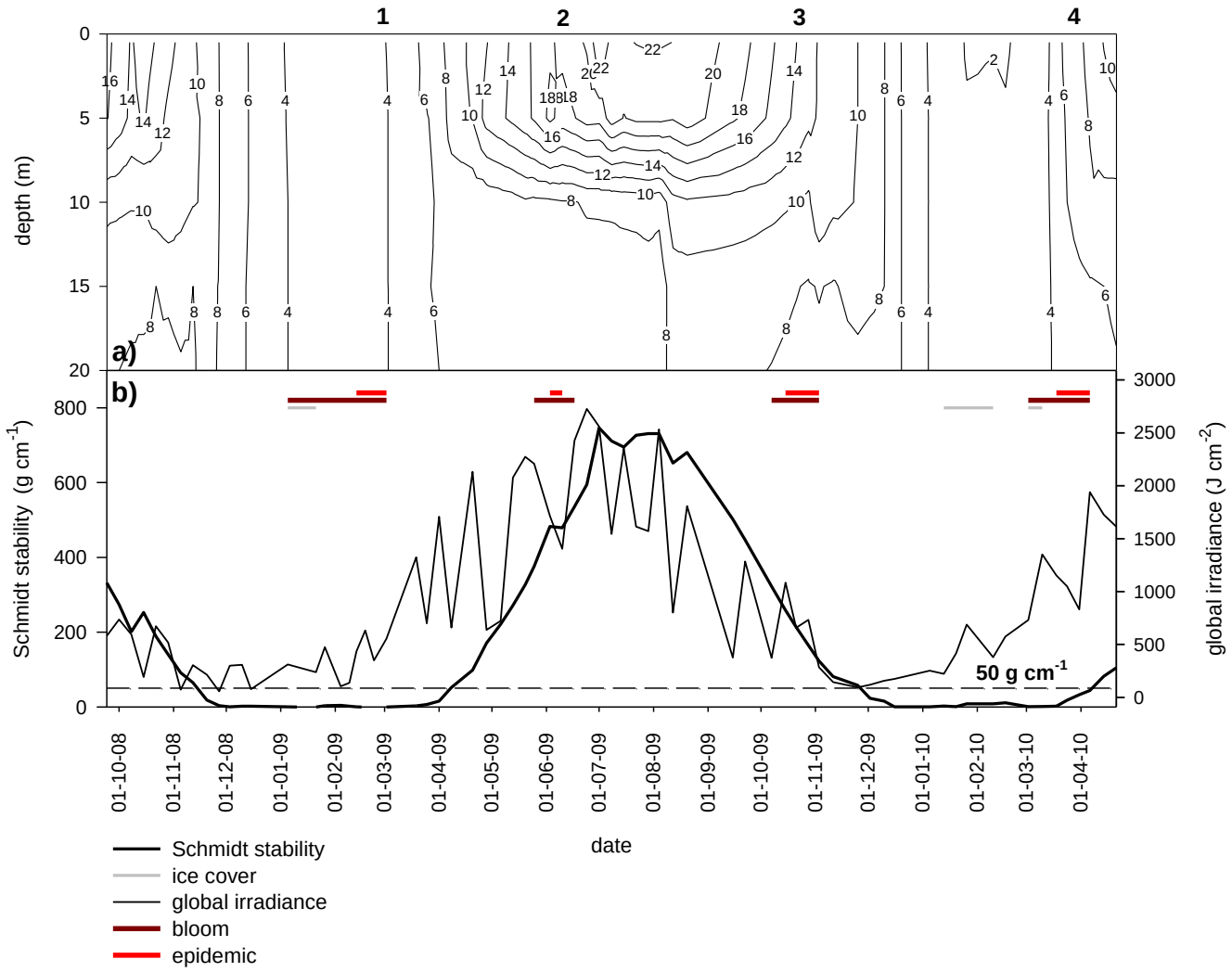

Fig 1

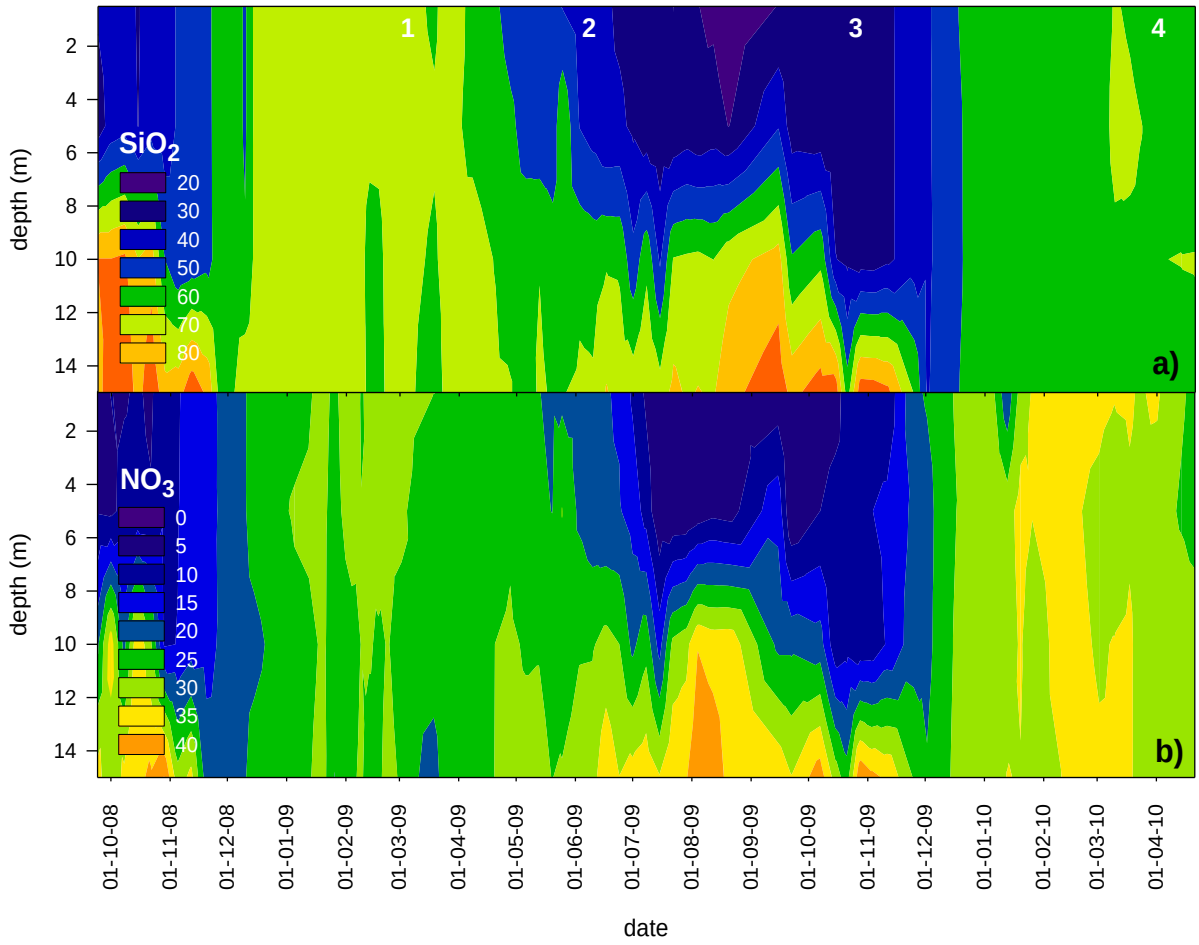
1
2
3
4
SiO2
20
30
40
50
60
70
80
a)
NO3
0
5
10
15
20
25
30
35
40
b)
depth (m)
depth (m)
2
4
6
8
10
12
14
01-10-08
01-11-08
01-12-08
01-01-09
01-02-09
01-03-09
01-04-09
01-05-09
01-06-09
01-07-09
01-08-09
01-09-09
01-10-09
01-11-09
01-12-09
01-01-10
01-02-10
01-03-10
01-04-10
date

Fig 2

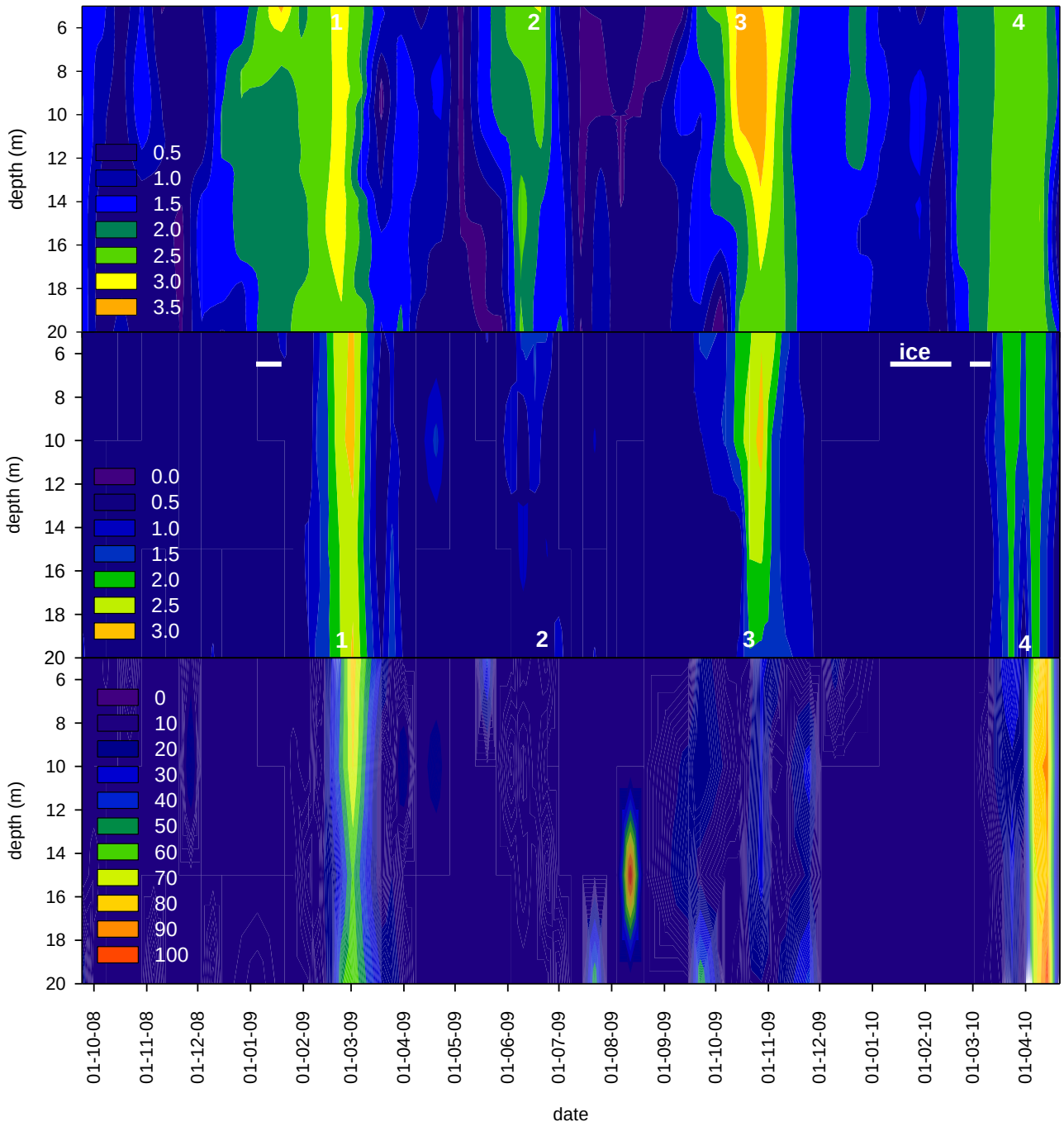
depth (m)
6
8
10
12
14
16
18
20
1
2
3
4
0.5
1.0
1.5
2.0
2.5
3.0
3.5
ice
0.0
0.5
1.0
1.5
2.0
2.5
3.0
0
10
20
30
40
50
60
70
80
90
100
01-10-08
01-11-08
01-12-08
01-01-09
01-02-09
01-03-09
01-04-09
01-05-09
01-06-09
01-07-09
01-08-09
01-09-09
01-10-09
01-11-09
01-12-09
01-01-10
01-02-10
01-03-10
01-04-10
date

Fig 3

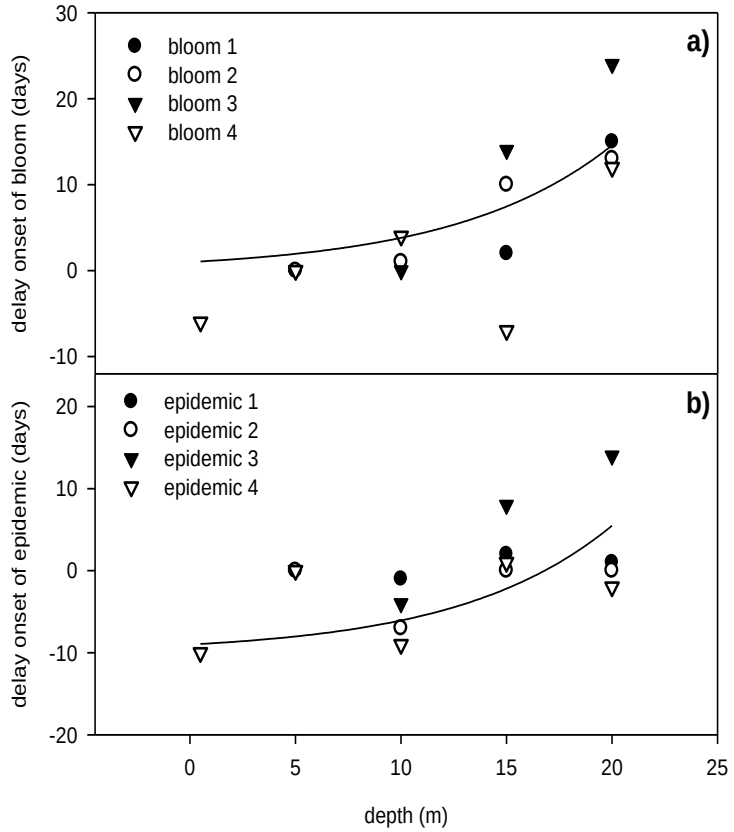
a)
bloom 1
bloom 2
bloom 3
bloom 4
delay onset of bloom (days)
30
20
10
0
-10
b)
epidemic 1
epidemic 2
epidemic 3
epidemic 4
delay onset of epidemic (days)
20
10
0
-10
-20
0
5
10
15
20
25
depth (m)

Fig 4

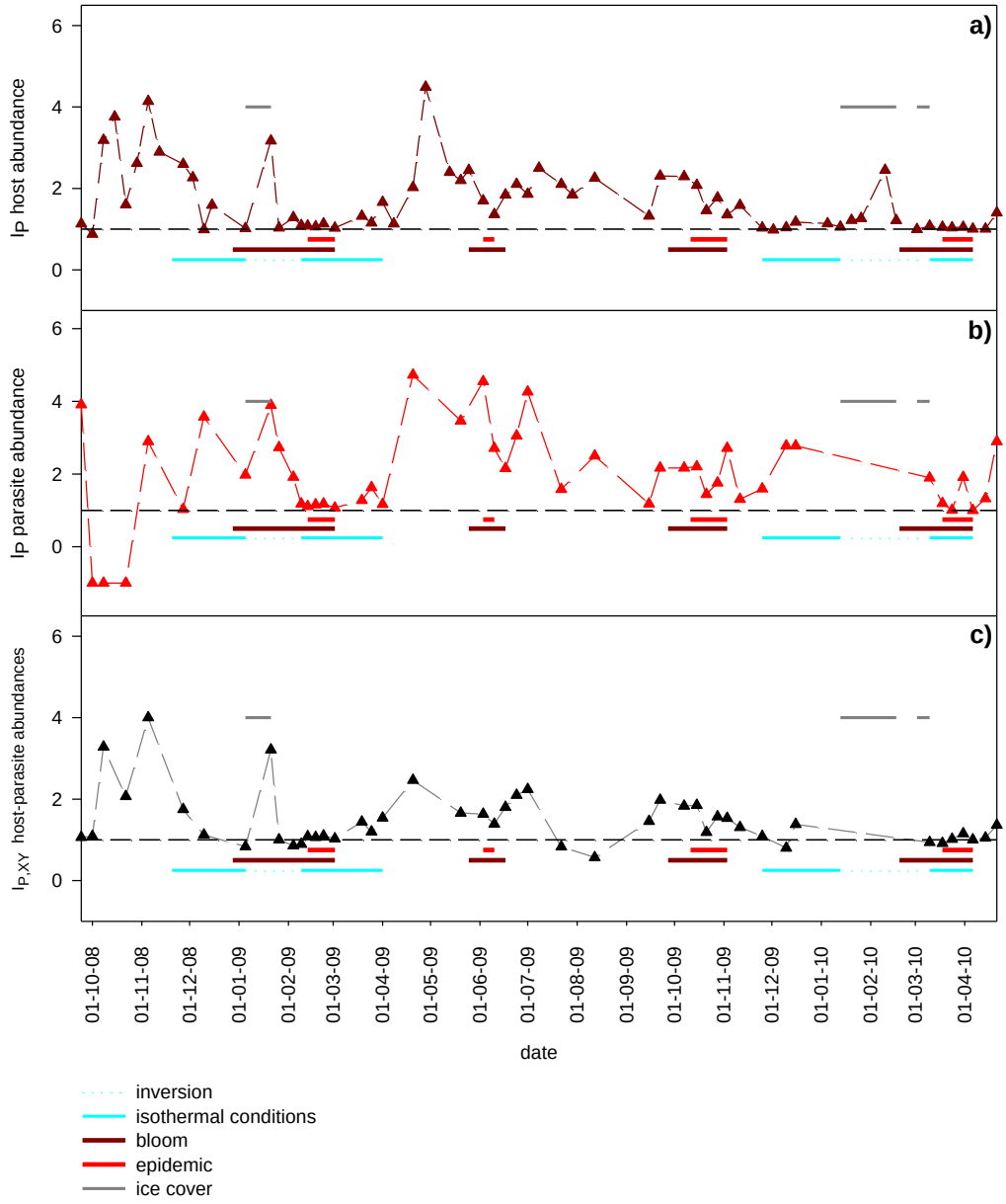
a)
b)
c)
I_P host abundance
I_P parasite abundance
$I_{P,XY}$ host-parasite abundances
0
2
4
6
01-10-08
01-11-08
01-12-08
01-01-09
01-02-09
01-03-09
01-04-09
01-05-09
01-06-09
01-07-09
01-08-09
01-09-09
01-10-09
01-11-09
01-12-09
01-01-10
01-02-10
01-03-10
01-04-10
date
inversion
isothermal conditions
bloom
epidemic
ice cover

Fig 5